J. Fluid Mech. (2010), *vol.* 654, *pp.* 281–303.
doi:10.1017/S0022112010000601

Fully nonlinear higher-order model equations for long internal waves in a two-fluid system

SUMA DEBSARMA[1], K. P. DAS[1] AND JAMES T. KIRBY[2]†

[1]Department of Applied Mathematics, University of Calcutta, 92 A.P.C. Road, Kolkata 700009, India

[2]Center for Applied Coastal Research, University of Delaware, Newark, DE 19716, USA

(Received 27 January 2009; revised 27 January 2010; accepted 31 January 2010;
first published online 11 May 2010)

Fully nonlinear model equations, including dispersive effects at one-order higher approximation than in the model of Choi & Camassa (*J. Fluid Mech.*, vol. 396, 1999, pp. 1–36), are derived for long internal waves propagating in two spatial horizontal dimensions in a two-fluid system, where the lower layer is of infinite depth. The model equations consist of two coupled equations for the displacement of the interface and the horizontal velocity of the upper layer at an arbitrary elevation, and they are correct to $O(\mu^2)$ terms, where μ is the ratio of thickness of the upper-layer fluid to a typical wavelength. For solitary waves propagating in one horizontal direction, the two coupled equations reduce to a single equation for the elevation of the interface. Solitary wave profiles obtained numerically from this equation for different wave speeds are in good agreement with computational results based on Euler's equations. A numerical approach for the propagation of solitary waves is provided in the weakly nonlinear case.

1. Introduction

The dynamics of internal waves in stratified fluid has attracted great attention due to their importance in near coastal dynamics. Recent observations show that large-amplitude internal waves are common phenomena in oceans (see e.g. Liu *et al.* 1998; Stanton & Ostrovsky 1998; Orr & Mignerey 2003; Zeng & Alpers 2004). An atlas of internal solitary-like waves and their properties in different ocean basins is available in Jackson (2004). Recently, Helfrich & Melville (2006) have given an extensive review of the properties of steady internal solitary waves and transient processes of wave generation and evolution, primarily from the point of view of weakly nonlinear theory of which the Korteweg–de Vries (KdV) equation is the most frequently used example.

Appropriate model equations are needed to describe the long internal waves mentioned above. Koop & Butler (1981) were the first to investigate whether weakly nonlinear model equations in a two-fluid system are appropriate for describing experimental results. They concluded that the weakly nonlinear KdV model equation performed fairly well over a wide range of amplitudes for configurations involving shallow depths in each layer. However, Grue *et al.* (1999) found that KdV theory departed from experiments and the Euler equations, when the wave amplitude over the thin layer depth exceeded 0.4, for moderate depth ratio. For deep-water configurations, Segur & Hammack (1982), using salt-stratified water, confirmed that

† Email address for correspondence: kirby@udel.edu

weakly nonlinear theory agrees poorly with experimental observation. However, it is true that fully nonlinear dispersive theory departs earlier from the Benjamin-Ono (BO) asymptote (infinitely deep lower layer) than when the lower-layer depth is finite, but large (see Fructus & Grue 2004, figure 5*b*, *c*). These observations have led to a continuing interest in the development of both weakly nonlinear and fully nonlinear model equations for two-fluid systems in both finite and infinite depth configurations. Recent examples include Choi & Camassa (1996*a*) and Lynett & Liu (2002) for weakly nonlinear waves and Choi & Camassa (1996*b*, 1999) for fully nonlinear waves. Choi & Camassa (1996*b*, 1999) derived fully nonlinear $O(\mu)$ model equations for internal waves in a two-fluid system; here μ is the ratio of the depth of the upper fluid to a typical wavelength of the internal wave. In a later paper, Camassa *et al.* (2006) investigated the region of validity of KdV and the formulation by Choi & Camassa (1999) for large-amplitude waves by comparing the solutions with direct solutions of the Euler equations using the formulation of Grue *et al.* (1999).

It has been known for a long while that Choi & Camassa (1999) model has relatively poor representation of dispersive effects, which has been documented in the paper by Ostrovsky & Grue (2003). In the present study, the highly nonlinear $O(\mu)$ model equations derived by Choi & Camassa (1996*b*, 1999) are extended to include $O(\mu^2)$ terms. The model described here is restricted to the limit of infinite lower-layer depth, but we allow for propagation in two horizontal spatial dimensions. Instead of using the depth averaged upper-layer velocity as a dependent variable, we use the horizontal velocity at an arbitrary elevation in the upper layer as the velocity variable. This approach was first introduced by Nwogu (1993) to derive a new form of Boussinesq equations in a single fluid layer, and was later followed by Wei *et al.* (1995) to derive fully nonlinear Boussinesq equations for surface waves, to the same order in approximation of dispersive effects as considered here. Extensions of this approach to higher order in dispersive properties may be found, for example, in Gobbi, Kirby & Wei (2000) and Madsen, Bingham & Liu (2002). The model equations we derive consist of two coupled equations for two variables, one of which is the elevation of the interface and the other is the horizontal velocity of the upper layer at an arbitrary elevation. The model equations derived here give a linear dispersion relation which agrees with the full linear dispersion relation to within the accuracy of a (2, 2) Padé approximation for the $\tanh x/x$ term appearing in the full expression. A reduced form of the model equations is obtained for propagation in one horizontal space dimension. In the limit of infinite lower-layer depth, the two reduced equations are found to be equivalent to (1) of Choi & Camassa (1996*b*) and to (4.17) and (4.18) of Choi & Camassa (1999) when $O(\mu^2)$ terms are neglected, and to (12) of Ruiz de Zárate *et al.* (2009) when $O(\mu^2)$ terms are retained, when the reduced equations are expressed in terms of depth averaged velocity of the upper layer.

For a solitary wave travelling with constant speed, the model equations are reduced to a single equation for the elevation of the interface, which is found to be the same as (13) of Choi & Camassa (1996*b*) when $O(\mu^2)$ terms are dropped. Numerical solutions for solitary wave profiles are obtained for different wave speeds. Results are also compared with the results obtained from full Euler equations algorithm described in Grue *et al.* (1999) for the case when the depth of lower fluid is 9 times and 24 times that of the upper fluid. It is found that the solitary wave profiles obtained from $O(\mu^2)$ order evolution equation are in better agreement with Euler's results than those obtained from $O(\mu)$ evolution equation of Choi & Camassa (1999), described in Camassa *et al.* (2006).

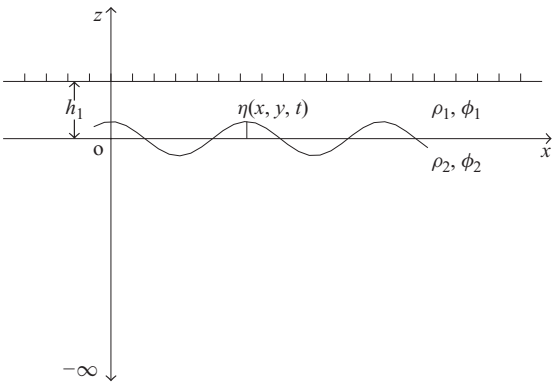

FIGURE 1. Fluid domain for two-fluid model with infinite lower-layer depth.

Finally, a numerical approach for studying one-way propagation in one horizontal dimension is described, following on the work of Nguyen & Dias (2008) in the weakly nonlinear case.

2. Derivation of the $O(\mu^2)$ model equations

We consider internal waves propagating at the interface of two inviscid incompressible fluids, where the upper fluid is of finite depth h_1, the lower fluid is of infinite depth and there is a rigid lid at the top of the upper fluid. (The rigid lid approximation is justified for internal wave motions having frequencies which are much lower than the frequency of a surface wave of comparable wavelength (see Phillips 1977, § 5.2.) The undisturbed interface of the two fluids is taken as the plane $z = 0$, the positive direction of z-axis pointing vertically upwards (figure 1). We assume the fluid to be inviscid and incompressible and the motion to be irrotational.

Following Choi & Camassa (1999), we non-dimensionalize relevant variables using

$$(x, y) = \frac{1}{L}(x^*, y^*), \quad z = \frac{z^*}{h_1}, \quad t = \frac{U_0}{L}t^*, \quad \phi_{1,2} = \frac{\phi^*_{1,2}}{\epsilon U_0 L}, \quad \eta = \frac{\eta^*}{\alpha}, \tag{2.1}$$

where asterisks denote dimensional forms. Here, (x, y) denotes horizontal position, η represents interface displacement and ϕ_i represents velocity potential in each layer. Additional scales include $U_0 = \sqrt{gh_1}$, L a typical wavelength of a long internal wave propagating in the two-layer fluid system, and α, a characteristic value of η. We introduce two parameters: $\mu = (h_1/L) \ll 1$, characterizing relative wavelength or frequency dispersion, and $\epsilon = \alpha/h_1 = O(1)$, characterizing nonlinearity.

The non-dimensional governing equations for the problem can then be written as

$$\phi_{1zz} + \mu^2\nabla^2\phi_1 = 0, \qquad \epsilon\eta < z < 1, \tag{2.2}$$

$$\phi_{1z} = 0, \qquad z = 1, \tag{2.3}$$

$$\eta_t + \epsilon\nabla\phi_1 \cdot \nabla\eta = \frac{1}{\mu^2}\phi_{1z}, \qquad z = \epsilon\eta \tag{2.4}$$

for the upper layer, and

$$\phi_{2zz} + \mu^2 \nabla^2 \phi_2 = 0, \qquad -\infty < z < \epsilon\eta, \tag{2.5}$$

$$\phi_2 \text{ bounded as } z \to -\infty, \tag{2.6}$$

$$\eta_t + \epsilon \nabla\phi_2 \cdot \nabla\eta = \frac{1}{\mu^2}\phi_{2z}, \qquad z = \epsilon\eta \tag{2.7}$$

for the lower layer. Matching pressure at the interface then gives

$$(1-R)\eta + \phi_{2t} - R\phi_{1t} + \frac{\epsilon}{2}(\nabla\phi_2)^2 + \frac{\epsilon}{2\mu^2}(\phi_{2z})^2 - \frac{\epsilon R}{2}(\nabla\phi_1)^2 - \frac{\epsilon R}{2\mu^2}(\phi_{1z})^2 = 0, \qquad z = \epsilon\eta, \tag{2.8}$$

where $R = \rho_1/\rho_2 \leqslant 1$.

Taking the Fourier transform of (2.2) and (2.3) with respect to x and y gives

$$\bar{\phi}_{1zz} - k^2\mu^2\bar{\phi}_1 = 0 \tag{2.9}$$

and

$$\bar{\phi}_{1z} = 0 \quad \text{at } z = 1, \tag{2.10}$$

where the Fourier transform of a function $f(x, y)$ with respect to x, y has been defined as

$$\bar{f} = \frac{1}{2\pi}\int\int_{-\infty}^{\infty} f(x, y) e^{i(k_x x + k_y y)}\, dx\, dy, \tag{2.11}$$

and where $\boldsymbol{k} = (k_x, k_y)$ is a wavenumber vector with $k = |\boldsymbol{k}|$.

The solution of (2.9) satisfying (2.10) is

$$\bar{\phi}_1 = \bar{A}\cosh\mu k(z-1), \tag{2.12}$$

$A = F^{-1}[\bar{A}]$ is the value of ϕ_1 at $z = 1$, where by F^{-1} we mean Fourier inversion. Expanding (2.12) in powers of μk, keeping terms up to any desired power of μ and then using Fourier inversion, we can express ϕ_1 in terms of the variable A. Instead, we shall express ϕ_1 in terms of a new variable $\phi_a(x, y)$, the value of ϕ_1 at $z = a$. The Fourier transform $\bar{\phi}_a$ of ϕ_a with respect to x, y can be obtained from (2.12) by setting $z = a$. We get the following expression for $\bar{\phi}_a$, the Fourier transform of $\phi_a = (\phi_1)_{z=a}$:

$$\bar{\phi}_a = \bar{A}\cosh\mu k(a-1). \tag{2.13}$$

The following equation is obtained after eliminating $\bar{A}$ between (2.12) and (2.13):

$$\bar{\phi}_1 = \bar{\phi}_a \frac{\cosh\mu k(z-1)}{\cosh\mu k(a-1)}. \tag{2.14}$$

Expanding (2.14) in powers of μk gives the following expression for $\bar{\phi}_1$, correct up to $O(\mu^2)$ terms:

$$\bar{\phi}_1 = \bar{\phi}_a + \frac{1}{2}\mu^2 k^2\{(z-1)^2 - B_2\}\bar{\phi}_a + O(\mu^4), \tag{2.15}$$

where

$$B_2 = (a-1)^2. \tag{2.16}$$

Fourier inversion of (2.15) gives the following expression for ϕ_1 expressed in terms of a new variable ϕ_a as desired:

$$\phi_1 = \phi_a - \frac{1}{2}\mu^2\{(z-1)^2 - B_2\}\nabla^2\phi_a + O(\mu^4). \tag{2.17}$$

For the potential of the lower layer, we take the Fourier transform of (2.5) and (2.6) with respect to x, y and get

$$\bar{\phi}_{2zz} - k^2\mu^2\bar{\phi}_2 = 0 \tag{2.18}$$

and

$$\bar{\phi}_2 \qquad \text{bounded as } z \to -\infty. \tag{2.19}$$

The solution of (2.18) satisfying (2.19) is

$$\bar{\phi}_2 = \bar{B}\mathrm{e}^{\mu k z}, \tag{2.20}$$

where $B = F^{-1}[\bar{B}]$ is the value of ϕ_2 at $z = 0$. Expanding (2.20) in ascending powers of μk, we get

$$\bar{\phi}_2 = \bar{B} + \mu k z\bar{B} + \frac{1}{2}\mu^2k^2z^2\bar{B} + \frac{1}{6}\mu^3k^3z^3\bar{B} + O(\mu^4). \tag{2.21}$$

This expression is valid for finite $|z|$ and is not uniformly valid for large $|z|$. As we need the value of $\bar{\phi}_2$ at $z = \eta$, i.e. at a finite value of $|z|$ and not for the whole range of $|z|$, the polynomial approximation for $\bar{\phi}_2$ given by (2.21) is sufficient for our purpose.

The Fourier inversion of (2.21) gives

$$\begin{aligned}\phi_2 &= B + \mu z F^{-1}[k\bar{B}] - \frac{1}{2}\mu^2z^2\nabla^2B + \frac{1}{6}\mu^3z^3F^{-1}[k^3\bar{B}] + O(\mu^4),\\ &= B - \mu z P[B] - \frac{1}{2}\mu^2z^2\nabla^2B + \frac{1}{6}\mu^3z^3\nabla^2(P[B]) + O(\mu^4),\end{aligned} \tag{2.22}$$

where P is the integral operator given by

$$P[\psi(x, y)] = \frac{1}{2\pi}\int\int_{-\infty}^{\infty}\frac{\psi(x', y')}{[(x'-x)^2 + (y'-y)^2]^{3/2}}\,\mathrm{d}x'\,\mathrm{d}y' \tag{2.23}$$

which follows from

$$\begin{aligned}F^{-1}[k\bar{B}] &= F^{-1}\left[\left(k_x^2 + k_y^2\right)\frac{\bar{B}}{k}\right],\\ &= -\nabla^2F^{-1}\left[\frac{\bar{B}}{k}\right],\\ &= -\nabla^2\frac{1}{2\pi}\int\int_{-\infty}^{\infty}\frac{B(x', y')}{\sqrt{(x'-x)^2 + (y'-y)^2}}\,\mathrm{d}x'\,\mathrm{d}y',\\ &= -\frac{1}{2\pi}\int\int_{-\infty}^{\infty}\frac{B(x', y')}{[(x'-x)^2 + (y'-y)^2]^{3/2}}\,\mathrm{d}x'\,\mathrm{d}y' = -P[B]\end{aligned} \tag{2.24}$$

by the use of convolution theorem and by the formula $F^{-1}[1/k] = 1/\sqrt{x^2 + y^2}$. The two-dimensional Fourier inversion formula like (2.24) were introduced in the papers by Grue (2002) and Clamond & Grue (2001) in more extended form in connection with fully nonlinear and fully dispersive interfacial waves.

We introduce here the integral operator given by

$$Q[\psi(x, y)] = \frac{1}{2\pi}\int\int_{-\infty}^{\infty}\frac{\psi(x', y')}{[(x'-x)^2 + (y'-y)^2]^{1/2}}\,\mathrm{d}x'\,\mathrm{d}y'. \tag{2.25}$$

It can easily be shown that

$$\nabla(Q[\psi(x, y)]) = \boldsymbol{H}[\psi(x, y)], \tag{2.26}$$

where $\boldsymbol{H}$ is a vector-valued two-dimensional operator given by

$$\boldsymbol{H}[\psi(x,y)] = \boldsymbol{i}_x \frac{1}{2\pi}\int\int_{-\infty}^{\infty} \frac{(x'-x)\psi(x',y')}{[(x'-x)^2+(y'-y)^2]^{3/2}}\,\mathrm{d}x'\,\mathrm{d}y' + \boldsymbol{i}_y \frac{1}{2\pi}\int\int_{-\infty}^{\infty} \frac{(y'-y)\psi(x',y')}{[(x'-x)^2+(y'-y)^2]^{3/2}}\,\mathrm{d}x'\,\mathrm{d}y' \quad (2.27)$$

The operator $\boldsymbol{H}$ will be needed in writing one of the two model equations at the end of this section.

Equation (2.22) shows that the terms containing odd powers of k in (2.21) produce terms expressed in terms of a Hilbert transform type operator when returning to physical space. This issue has previously been discussed and pursued by, for example, Choi & Camassa (1996*b*, 1999) in connection with internal waves and by Bingham & Agnon (2005) in connection with Boussinesq type formulation.

The $O(\mu^2)$ highly nonlinear model equations can now be obtained from (2.4), (2.7) and (2.8) after substituting for ϕ_1 and ϕ_2 from (2.17) and (2.22), respectively. The following equation is obtained after integrating (2.2) with respect to z between the limits $\epsilon\eta$ and 1 and then using (2.4):

$$-\frac{\partial\eta}{\partial t} + \nabla\cdot\int_{\epsilon\eta}^{1}\nabla\phi_1\,\mathrm{d}z = 0. \quad (2.28)$$

Substituting here for ϕ_1 given by (2.17) and then performing the integration gives the following equation, which constitutes one of the three model equations we are going to derive:

$$\frac{\partial\eta}{\partial t} - \nabla\cdot(h\boldsymbol{u}_a) + \frac{1}{2}\mu^2\nabla\cdot\left\{h\left(\frac{1}{3}h^2 - B_2\right)\nabla(\nabla\cdot\boldsymbol{u}_a)\right\} = 0, \quad (2.29)$$

where we have set

$$\boldsymbol{u}_a = \nabla\phi_a \quad (2.30)$$

and where $h = 1-\epsilon\eta$.

Integrating (2.5) with respect to z between the limits $-\infty$ and $\epsilon\eta$ and then using (2.7), we get

$$\frac{\partial\eta}{\partial t} + \nabla\cdot\int_{-\infty}^{\epsilon\eta}\nabla\phi_2\,\mathrm{d}z = 0. \quad (2.31)$$

In this equation we cannot substitute for ϕ_2 given by (2.22) and integrate term by term with respect to z as one of the limits of integration is $-\infty$. To remove this difficulty we proceed as follows. We define a vector-valued function $\boldsymbol{f}(z)$ as

$$\boldsymbol{f}(z) = \int_{-\infty}^{z}\nabla\phi_2\,\mathrm{d}z. \quad (2.32)$$

Then, (2.31) can be written as

$$\frac{\partial\eta}{\partial t} + \nabla\cdot(\boldsymbol{f})_{z=\epsilon\eta} = 0. \quad (2.33)$$

Taking the Fourier transform of (2.32) with respect to x and y gives

$$\bar{\boldsymbol{f}} = -\mathrm{i}\boldsymbol{k}\int_{-\infty}^{z}\bar{\phi}_2\,\mathrm{d}z. \quad (2.34)$$

Substituting for $\bar{\phi}_2$ given by (2.20) and then integrating with respect to z gives

$$\mu \bar{\boldsymbol{f}} = -\mathrm{i}\frac{\boldsymbol{k}}{k}\bar{B}\mathrm{e}^{\mu k z} \tag{2.35}$$

or

$$\mu \bar{\boldsymbol{f}} = -\mathrm{i}\frac{\boldsymbol{k}}{k}\bar{B} - \mathrm{i}\boldsymbol{k}\mu z\bar{B} - \frac{1}{2}\mathrm{i}\mu^2 k^2 z^2 \frac{\boldsymbol{k}}{k}\bar{B} + O(\mu^3) \tag{2.36}$$

after expanding $\mathrm{e}^{\mu k z}$ in ascending powers of μk. Fourier inversion of (2.36) gives

$$\mu \boldsymbol{f} = \nabla(Q[B]) + \mu z \nabla B - \frac{1}{2}\mu^2 z^2 \nabla(\nabla^2(Q[B])) + O(\mu^3) \tag{2.37}$$

by the use of the result

$$F^{-1}\left[\frac{\bar{B}}{k}\right] = \frac{1}{2\pi}\int\int_{-\infty}^{\infty} \frac{B(x', y')}{\sqrt{(x'-x)^2 + (y'-y)^2}}\,\mathrm{d}x'\,\mathrm{d}y' = Q[B],$$

according to (2.24) and (2.25).

Multiplying (2.33) by μ, substituting for $\mu \boldsymbol{f}$ using (2.37) and keeping terms up to $O(\mu^2)$ gives

$$\mu\frac{\partial \eta}{\partial t} + P[B] + \mu\epsilon\nabla\cdot(\eta\nabla B) - \frac{1}{2}\mu^2\epsilon^2\nabla\cdot\{\eta^2\nabla(P[B])\} = 0, \tag{2.38}$$

where the relation (2.25) has been used. Equation (2.38) is the second of the three $O(\mu^2)$ model equations, and represents depth-integrated volume conservation in the lower layer. The third equation will now be derived from (2.8). Substituting in this equation the expressions for ϕ_1 and ϕ_2 given respectively by (2.17) and (2.22), we get the following equation correct to $O(\mu^2)$ terms:

$$\begin{aligned}
&(1-R)\eta + B_t - R\phi_{at} + \frac{1}{2}\epsilon(\nabla B)^2 - \frac{1}{2}\epsilon R(\nabla\phi_a)^2 + \frac{1}{2}\epsilon(P[B])^2 \\
&\quad + \mu\epsilon\eta\{-P[B_t] - \epsilon(\nabla B)\cdot\nabla(P[B]) + \epsilon P[B]\nabla^2 B\} \\
&\quad + \frac{1}{2}\mu^2\left[-\epsilon^2\eta^2\{\nabla^2 B_t - \epsilon(\nabla P[B])^2 + \epsilon(\nabla B)\cdot\nabla(\nabla^2 B) - \epsilon(\nabla^2 B)^2 + \epsilon(P[B])\nabla^2(P[B])\}\right. \\
&\quad \left. + R(h^2 - B_2)\nabla^2\phi_{at} + \epsilon R(h^2 - B_2)(\nabla\phi_a)\cdot\nabla(\nabla^2\phi_a) - \epsilon R h^2(\nabla^2\phi_a)^2\right] = 0.
\end{aligned} \tag{2.39}$$

The three equations (2.29), (2.38) and (2.39) constitute the $O(\mu^2)$ model equations where the neglected terms are of $O(\mu^3)$. The last two equations can be simplified considerably due to the estimate

$$P[B] = O(\mu) \tag{2.40}$$

that can be obtained from (2.38). Due to the estimate (2.40), (2.38) and (2.39) can be reduced to the following equations, where $O(\mu^3)$ and higher-order small terms are neglected:

$$\mu\frac{\partial \eta}{\partial t} + P[B] + \mu\epsilon\nabla\cdot(\eta\nabla B) = 0, \tag{2.41}$$

$$\begin{aligned}
&(1-R)\eta + B_t - R\phi_{at} + \frac{1}{2}\epsilon(\nabla B)^2 - \frac{1}{2}\epsilon R(\nabla\phi_a)^2 + \frac{1}{2}\epsilon(P[B])^2 - \mu\epsilon\eta(P[B_t]) + \frac{1}{2}\mu^2 \\
&\quad \times\left[R(h^2 - B_2)\nabla^2\phi_{at} + \epsilon R(h^2 - B_2)(\nabla\phi_a)\cdot\nabla(\nabla^2\phi_a) - \epsilon R h^{(}\nabla^2\phi_a)^2\right] = 0.
\end{aligned} \tag{2.42}$$

We now express B in terms of η using (2.41), so that the model equations can involve only two unknowns η and $\boldsymbol{u}_a$ governed by two equations. Taking the Fourier transform of (2.41), we can express $\bar{B}$ as

$$\bar{B} = \frac{\mu}{k}\bar{\eta}_t - \frac{\mathrm{i}\mu\epsilon}{k}\boldsymbol{k}\cdot F[\eta\nabla B] + O(\mu^3), \tag{2.43}$$

the Fourier inversion of which gives

$$B = \mu Q[\eta_t] + \mu\epsilon Q[\nabla\cdot(\eta\nabla B)] + O(\mu^3), \tag{2.44}$$

where Q is an integral operator given by (2.25).

Inverting (2.44) for B gives

$$B = \mu Q[\eta_t] + \mu^2\epsilon Q[\nabla\cdot\{\eta\nabla(Q[\eta_t])\}] + O(\mu^3). \tag{2.45}$$

Taking the gradient of (2.42) and then eliminating B by the use of (2.45), the following equation correct to $O(\mu^2)$ terms is obtained, where we use the relation (2.26):

$$\begin{aligned}
&(1-R)\nabla\eta + \mu\boldsymbol{H}[\eta_{tt}] + \mu^2\epsilon\boldsymbol{H}[\nabla\cdot\{\eta_t\boldsymbol{H}[\eta_t]\}] + \mu^2\epsilon\boldsymbol{H}[\nabla\cdot\{\eta\boldsymbol{H}[\eta_{tt}]\}] - R\boldsymbol{u}_{at}\\
&\quad -\epsilon R(\boldsymbol{u}_a\cdot\nabla)\boldsymbol{u}_a + \mu^2\epsilon\{\boldsymbol{H}[\eta_t]\cdot\nabla\}\boldsymbol{H}[\eta_t] + \mu^2\epsilon\eta_t\nabla\eta_t + \mu^2\epsilon\nabla(\eta\eta_{tt})\\
&\quad +\frac{1}{2}\mu^2 R\nabla\{(h^2-B_2)\nabla\cdot\boldsymbol{u}_{at}\} + \frac{1}{2}\mu^2\epsilon R\nabla\{(h^2-B_2)\boldsymbol{u}_a\cdot\nabla(\nabla\cdot\boldsymbol{u}_a)\}\\
&\quad -\frac{1}{2}\mu^2\epsilon R\nabla\{h^2(\nabla\cdot\boldsymbol{u}_a)^2\} = 0,
\end{aligned} \tag{2.46}$$

where $\boldsymbol{u}_a$ is defined in (2.30). The two coupled equations (2.29) and (2.46) in terms of the two dependent variables η and $\boldsymbol{u}_a$ constitute the $O(\mu^2)$ model equations for highly nonlinear internal waves in a two-layer fluid system, where the lower layer is of infinite depth.

The two model equations (2.29) and (2.46) can be written in a form more suitable for numerical time-domain solution. From these two equations we get, by successive approximation, the following $O(\mu)$ estimates of η_t, $\boldsymbol{u}_{at}$ and η_{tt} which do not contain time derivatives:

$$\eta_t = A + O(\mu^2), \qquad \boldsymbol{u}_{at} = \boldsymbol{U} + O(\mu), \qquad \eta_{tt} = A_1 + \mu A_2 + O(\mu^2), \tag{2.47}$$

where

$$\left.\begin{aligned}
A &= \nabla\cdot(h\boldsymbol{u}_a),\\
\boldsymbol{U} &= \left(\frac{1-R}{R}\right)\nabla\eta - \epsilon(\boldsymbol{u}_a\cdot\nabla)\boldsymbol{u}_a,\\
A_1 &= -\epsilon\nabla\cdot\{\boldsymbol{u}_a\nabla\cdot(h\boldsymbol{u}_a)\} + \left(\frac{1-R}{R}\right)\nabla\cdot(h\nabla\eta) - \epsilon\nabla\cdot\{h(\boldsymbol{u}_a\cdot\nabla)\boldsymbol{u}_a\},\\
A_2 &= -\frac{\epsilon}{R}\nabla\cdot\{h\boldsymbol{H}[\nabla\cdot\{(\nabla\cdot(h\boldsymbol{u}_a))\boldsymbol{u}_a\}]\} + \left(\frac{1-R}{R^2}\right)\nabla\cdot\{h\boldsymbol{H}[\nabla\cdot(h\nabla\eta)]\}\\
&\quad -\frac{\epsilon}{R}\nabla\cdot\{h\boldsymbol{H}[\nabla\cdot\{h(\boldsymbol{u}_a\cdot\nabla)\boldsymbol{u}_a\}]\}.
\end{aligned}\right\} \tag{2.48}$$

Substituting the expressions for η_t, $\boldsymbol{u}_{at}$ and η_{tt} given by (2.47) in the model equations (2.29) and (2.46) leads to the following forms which are suitable for numerical time-domain solution:

$$\eta_t = A - \frac{1}{2}\mu^2\nabla\cdot\left\{h\left(\frac{1}{3}h^2 - B_2\right)\nabla(\nabla\cdot\boldsymbol{u}_a)\right\} \tag{2.49}$$

and

$$\boldsymbol{u}_{at} = \left(\frac{1-R}{R}\right)\nabla\eta - \epsilon(\boldsymbol{u}_a\cdot\nabla)\boldsymbol{u}_a + \frac{\mu}{R}\boldsymbol{H}[A_1] + \frac{\mu^2}{R}\boldsymbol{H}[A_2] + \frac{\mu^2\epsilon}{R}\boldsymbol{H}[\nabla\cdot\{A\boldsymbol{H}[A]\}]$$
$$+ \frac{\mu^2\epsilon}{R}\boldsymbol{H}[\nabla\cdot\{\eta\boldsymbol{H}[A_1]\}] + \frac{\mu^2\epsilon}{R}\{\boldsymbol{H}[A]\cdot\nabla\}\boldsymbol{H}[A] + \frac{\mu^2\epsilon}{R}A\nabla A + \frac{\mu^2\epsilon}{R}\nabla(\eta A_1)$$
$$+ \frac{1}{2}\mu^2\nabla\{(h^2-B_2)\nabla\cdot\boldsymbol{u}\} + \frac{1}{2}\mu^2\epsilon\nabla\{(h^2-B_2)\boldsymbol{u}\cdot\nabla(\nabla\cdot\boldsymbol{u}_a)\}$$
$$- \frac{1}{2}\mu^2\epsilon\nabla\{h^2(\nabla\cdot\boldsymbol{u}_a)^2\}. \tag{2.50}$$

3. Propagation in one horizontal space dimension

In this section we find the reduced form of the two equations (2.29) and (2.46) when propagation takes place in one horizontal space dimension, which we take as x-axis.

It can be shown that when ψ does not depend on y, then

$$\boldsymbol{H}[\psi(x)] = \boldsymbol{i}_x H[\psi(x)], \tag{3.1}$$

where H is the Hilbert transform operator given by

$$H[\psi(x)] = \frac{1}{\pi}\int_{-\infty}^{\infty}\frac{\psi(x')}{x'-x}\,\mathrm{d}x'. \tag{3.2}$$

Also, since in this particular case the dependent variables do not depend on y, we get

$$\boldsymbol{u}_a = \nabla\phi_a = \boldsymbol{i}_x\phi_{ax} = \boldsymbol{i}_x u, \tag{3.3}$$

where the subscript a is subsequently dropped. Equation (2.29) then reduces to

$$\eta_t - (hu)_x + \frac{1}{2}\mu^2\left\{h\left(\frac{h^2}{3} - B_2\right)u_{xx}\right\}_x = 0, \tag{3.4}$$

where $O(\mu^3)$ terms are neglected.

The y-component of (2.46) vanishes identically, while its x-component becomes

$$(1-R)\eta_x + \mu H[\eta_{tt}] + \mu^2\epsilon H[\{\eta_t H[\eta_t]\}_x] + \mu^2\epsilon H[\{\eta H[\eta_{tt}]\}_x] - Ru_t$$
$$+ \mu^2\epsilon H[\eta_t]\{H[\eta_t]\}_x - \epsilon Ruu_x + \mu^2\epsilon\eta_t\eta_{xt} + \mu^2\epsilon(\eta\eta_{tt})_x$$
$$+ \frac{1}{2}\mu^2 R\{(h^2-B_2)u_{xt}\}_x + \frac{1}{2}\mu^2\epsilon R\{(h^2-B_2)uu_{xx}\}_x - \frac{1}{2}\mu^2\epsilon R\{h^2u_x^2\}_x = 0, \tag{3.5}$$

where $O(\mu^3)$ terms are neglected.

Therefore, when propagation takes place in one horizontal space dimension, the coupled equations (3.4) and (3.5) constitute the $O(\mu^2)$ model equation for propagation of highly nonlinear internal waves in a two-layer fluid system in which the lower layer is of infinite depth.

The coupled equations (3.4) and (3.5) assume the following form when $O(\mu^2)$ terms are neglected:

$$\eta_t - (hu)_x = 0, \tag{3.6}$$
$$(1-R)\eta_x + \mu H[\eta_{tt}] - R(u_t + \epsilon uu_x) = 0. \tag{3.7}$$

If we write these two equations in dimensional form after writing $1/R = \rho$ and taking $a = h_1$, $L = h_1$ then they are equivalent to (1) of Choi & Camassa (1996*b*) and (4.17),

(4.18) of Choi & Camassa (1999), since their $\bar{u}_1$ can be identified with u of the present paper to within errors of $O(\mu^2)$.

The coupled equations (3.4) and (3.5) correct to $O(\mu^2)$ terms, when written in terms of depth-averaged horizontal velocity of the upper-layer fluid, are equivalent to the recently derived equations (12) of Ruiz de Zárate *et al.* (2009) for the case of infinite depth fluid. From (2.17) we find that the horizontal velocity $u_1 = \phi_{1x}$ of the upper fluid is

$$u_1 = u(x) - \frac{1}{2}\mu^2\{(z-1)^2 - B_2\}u_{xx} + O(\mu^4). \tag{3.8}$$

Hence, the depth-averaged velocity $\bar{u}_1$ is

$$\bar{u}_1 = \frac{1}{1-\epsilon\eta}\int_{\epsilon\eta}^{1} u_1 \,\mathrm{d}z = u - \frac{1}{2}\mu^2\left(\frac{1}{3}h^2 - B_2\right)u_{xx} + O(\mu^4). \tag{3.9}$$

Inverting this equation for u, we get

$$u = \bar{u}_1 + \frac{1}{2}\mu^2\left(\frac{1}{3}h^2 - B_2\right)\bar{u}_{1xx} + O(\mu^4). \tag{3.10}$$

Substituting the expression for u given by (3.10) in (3.4), we get

$$\eta_t - (h\bar{u}_1)_x = 0, \tag{3.11}$$

which is equivalent to the first of the two equations in (12) of Ruiz de Zárate *et al.* (2009) for infinite depth fluid. Next, we substitute the same expression for u given by (3.10) in (3.5) and arrive at the equation

$$\begin{aligned}\bar{u}_{1t} + \epsilon\bar{u}_1\bar{u}_{1x} + \left(1 - \frac{1}{R}\right)\eta_x = {} & \frac{\mu}{R}H[h\bar{u}]_{xt} + \frac{\mu^2}{3h}(h^3G)_x + \frac{\mu^2\epsilon}{R}\left[\eta(h\bar{u}_1)_{xt} + \frac{1}{2}[(h\bar{u}_1)_x]^2\right]_x \\ & + \frac{\mu^2\epsilon}{R}H[\eta H[h\bar{u}_1]_x]_{xt} + \frac{\mu^2\epsilon}{2R}[(H[h\bar{u}_1]_x)^2]_x + O(\mu^3)\end{aligned} \tag{3.12}$$

with

$$G = \bar{u}_{1xt} + \epsilon\bar{u}_1\bar{u}_{1xx} - \bar{u}_{1x}^2, \tag{3.13}$$

which is equivalent to the second of the two equations in (12) of Ruiz de Zárate *et al.* (2009).

4. Linear dispersion relation

In this section we find the linear dispersion relation from the two model equations (2.29) and (2.46). Firstly, we write below the full linear dispersion relation that can be obtained from the linearized form of the governing equations (2.2)–(2.8) after assuming space–time dependence of the dependent variables to be of the form $\exp \mathrm{i}(\boldsymbol{k}\cdot\boldsymbol{r} - \omega t)$. The phase speed resulting from the full linear problem is denoted by c_E and is given by

$$c_E^2 = \left(\frac{\omega}{k}\right)^2 = \frac{(1-R)T}{\mu k(R+T)}, \qquad T = \tanh\mu k. \tag{4.1}$$

For very long waves, i.e. for $\mu \to 0$, the above dispersion relation simplifies to

$$c_{LW}^2 = \frac{1-R}{R}. \tag{4.2}$$

Choi & Camassa (1999) give the dispersion relation for their model in (4.41). In the infinitely deep-water ($kh_2 \to \infty$) limit and in dimensionless form, this reduces to

$$c_{CC}^2 = \frac{1-R}{R+\mu k}. \tag{4.3}$$

Choi & Camassa (1999) point out that this expression is asymptotically equivalent to the BO dispersion relation

$$c_{BO}^2 = \frac{(1-R)}{R}\left(1-\frac{\mu k}{2R}\right)^2, \tag{4.4}$$

which follows from (2.9) in Choi & Camassa (1999). It is seen below that (4.3) and (4.4) diverge fairly rapidly for realistic ranges of wavelengths, indicating that (4.3) should be thought of as the proper expression for the model equations by Choi & Camassa (1999).

Turning to the present model, the linearized form of (2.29) is

$$\eta_t - P_a + \frac{1}{2}\mu^2\left(\frac{1}{3}-B_2\right)\nabla^2 P_a = 0, \tag{4.5}$$

where we have set

$$\nabla \cdot \boldsymbol{u}_a = P_a. \tag{4.6}$$

Next, taking the divergence of the linearized form of (2.46), we get

$$(1-R)\nabla^2\eta + \frac{\mu}{2\pi}\nabla^2 \int\int_{-\infty}^{\infty} \frac{\eta_{tt}(x', y')}{[(x'-x)^2+(y'-y)^2]^{1/2}}\,\mathrm{d}x'\,\mathrm{d}y' - RP_{at} + \frac{1}{2}\mu^2 R(1-B_2)\nabla^2 P_{at} = 0, \tag{4.7}$$

where we have used (4.6). Assuming space–time dependence of η and P_a to be of the form $\exp \mathrm{i}(\boldsymbol{k}\cdot\boldsymbol{r}-\omega t)$, (4.5) and (4.9) produce, as shown in Appendix A, the linear dispersion relation for the present model

$$c^2 = \frac{(1-R)T_{approx}}{\mu k(R+T_{approx})}; \qquad T_{approx} = \mu k \frac{1+\frac{1}{2}\left(\frac{1}{3}-B_2\right)\mu^2 k^2}{1+\frac{1}{2}(1-B_2)\mu^2 k^2}, \tag{4.8}$$

where T_{approx} represents an approximation to the tanh function appearing in (4.1). The free parameter B_2 can be chosen by forcing T_{approx} to correspond to the (2,2) Padé approximant

$$T_{approx} \to T_{Padé} = \mu k \frac{1+\frac{1}{15}\mu^2 k^2}{1+\frac{2}{5}\mu^2 k^2}, \tag{4.9}$$

which follows if we take $B_2 = 1/5$, which gives $(a-1)^2 = 1/5$, or $a = 1-1/\sqrt{5} = 0.5528$, corresponding to a reference elevation for u or ϕ_1 in the upper layer slightly above the mid depth of the layer.

Figure 2 displays dispersion relation results for a density ratio $\rho = 1/R = 1.05$ and a range of relative upper-layer depths $0 < \mu k < 5$, which covers the range from shallow to deep upper-layer depth relative to the interfacial wavelength. In figure 2(*a*), results for c^2 for the present theory are shown together with long wave, BO and Choi &

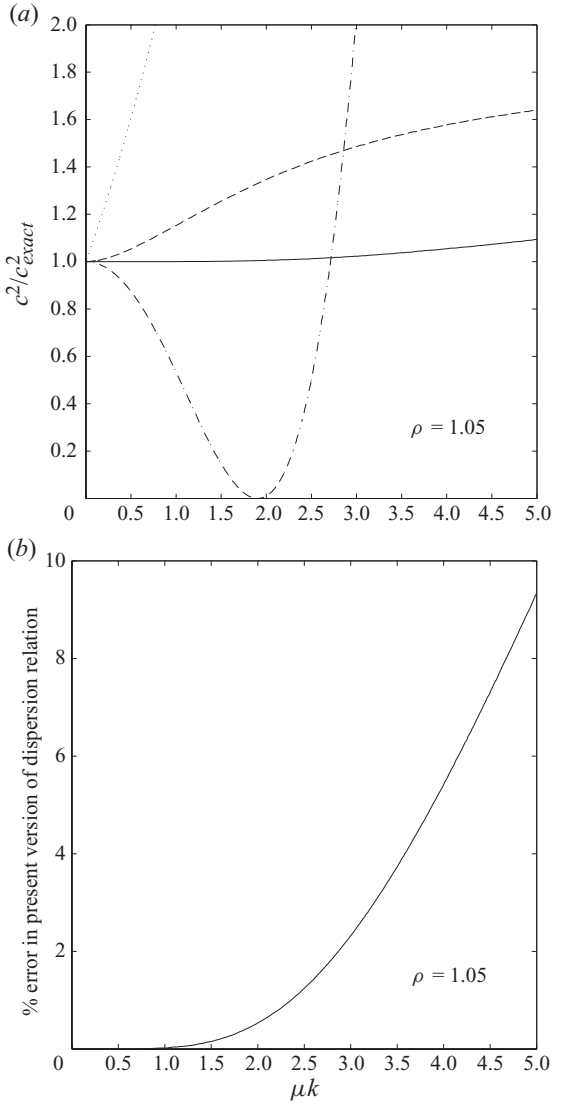

FIGURE 2. Normalized phase speed squared versus wavenumber for $\rho = 1/R = 1.05$. (*a*) Values of c^2 normalized by exact linear theory c_E^2 for the present theory (solid line), Choi & Camassa (1999) (dashed line), BO (dash-dot line) and long wave theory (dotted line). (*b*) Per cent error in c^2 for the present theory.

Camassa (1999) results, each of which have been normalized by the full linear theory result (4.1). The long wave result is seen to deviate rapidly from the exact solution. The improvement afforded by BO and Choi & Camassa (1999) results is only slight, and the two results then diverge in opposite directions, with the BO result breaking down for $\mu k \geqslant 2R$. In contrast, the dispersion relation predicted by the present $O(\mu^2)$ theory is relatively robust over a wide range of upper-layer depths. Figure 2(*b*) shows the per cent error in predicted phase speed squared for the present theory, which is typically less than 1 % for a reasonably wide range of upper-layer depths.

5. Travelling wave solution

For waves of finite amplitude propagating along x-axis with a constant velocity U, we substitute $\eta = \eta(X)$ and $u = u(X)$, with $X = x - Ut$ in the coupled equations (3.4) and (3.5), which are the $O(\mu^2)$ model equations for propagation in one horizontal space dimension. The two equations then assume the following form, where $O(\mu^3)$ terms are neglected:

$$-U\eta_X - (hu)_X + \frac{1}{2}\mu^2\left\{h\left(\frac{1}{3}h^2 - B_2\right)u_{XX}\right\}_X = 0, \tag{5.1}$$

$$\begin{aligned}(1-R)\eta_X &+ \mu U^2 H[\eta_{XX}] + \mu^2\epsilon U^2 H[\{\eta_X H[\eta_X]\}_X] + \mu^2\epsilon U^2 H[\{\eta H[\eta_{XX}]\}_X] \\ &+ RUu_X + \mu^2\epsilon U^2\{H[\eta_X]\partial_X\}H[\eta_X] - \epsilon Ruu_X + \mu^2\epsilon U^2\eta_X\eta_{XX} + \mu^2\epsilon(\eta\eta_{XX})_X \\ &- \frac{1}{2}\mu^2 RU\{(h^2 - B_2)u_{XX}\}_X + \frac{1}{2}\mu^2\epsilon R\{(h^2 - B_2)uu_{XX}\}_X - \frac{1}{2}\mu^2\epsilon R\{h^2u_X^2\}_X = 0.\end{aligned} \tag{5.2}$$

Terms involving repeated Hilbert transform operator in (5.2) are not new here as similar terms appear in (3.6) of Clamond & Grue (2001). Integrating (5.1) and (5.2) once and assuming that η, u and their derivatives vanish at $|X| \to \infty$, which are the requirements for a solitary wave, we get

$$-U\eta - hu + \frac{1}{2}\mu^2 h\left(\frac{1}{3}h^2 - B_2\right)u_{XX} = 0 \tag{5.3}$$

and

$$\begin{aligned}(1-R)\eta &+ \mu U^2 H[\eta_X] + \mu^2\epsilon U^2 H[\eta_X H[\eta_X]] + \mu^2\epsilon U^2 H[\eta H[\eta_{XX}]] \\ &+ RUu + \frac{1}{2}\mu^2\epsilon U^2\{H[\eta_X]\}^2 - \frac{1}{2}\epsilon Ru^2 + \frac{1}{2}\mu^2\epsilon U^2\eta_X^2 + \mu^2\epsilon\eta_{XX} \\ &- \frac{1}{2}\mu^2 RU(h^2 - B_2)u_{XX} + \frac{1}{2}\mu^2\epsilon R(h^2 - B_2)uu_{XX} - \frac{1}{2}\mu^2\epsilon Rh^2u_X^2 = 0.\end{aligned} \tag{5.4}$$

Inverting (5.3) for u gives (correct to $O(\mu^2)$ terms)

$$u = \frac{-U\eta}{h} - \frac{1}{2}\mu^2 U\left(\frac{1}{3}h^2 - B_2\right)\left(\frac{\eta}{h}\right)_{XX}. \tag{5.5}$$

Substituting this expression for u in (5.4), the following equation is obtained correct to $O(\mu^2)$ terms determining η:

$$\begin{aligned}(1-R)\eta &- \frac{RU^2\eta}{h^2} + \frac{\epsilon RU^2\eta^2}{2h^2} + \mu U^2\frac{\mathrm{d}}{\mathrm{d}X}H[\eta] \\ &+ \mu^2 U^2\left(\epsilon\eta + \frac{R}{3h}\right)\frac{\mathrm{d}^2\eta}{\mathrm{d}X^2} + \frac{1}{2}\mu^2\epsilon U^2\left(1 + \frac{R}{3h^2}\right)\left(\frac{\mathrm{d}\eta}{\mathrm{d}X}\right)^2 \\ &+ \frac{1}{2}\mu^2\epsilon U^2\left\{\frac{\mathrm{d}}{\mathrm{d}X}H[\eta]\right\}^2 + \mu^2\epsilon U^2\frac{\mathrm{d}}{\mathrm{d}X}H\left[\eta\frac{\mathrm{d}}{\mathrm{d}X}H[\eta]\right] = 0.\end{aligned} \tag{5.6}$$

If in the relation (2.1) introduced to write the governing equations in dimensionless form we replace U_0 by $c_0 = \sqrt{gh_1(1-R)/R}$, the velocity of a very long internal wave, and α by h_1, then (5.6) can be written as follows, where η and U represent dimensionless quantities η^*/h_1 and U^*/c_0, and where we set $\rho = 1/R$:

$$-\frac{\eta}{U^2} + \frac{1}{2(1-\eta)^2} - \frac{1}{2} - \mu\rho H[\eta_X] = \mu^2 F(\eta, \eta_X, \eta_{XX}), \tag{5.7}$$

where

$$F(\eta, \eta_X, \eta_{XX}) = \frac{1}{2}\left(\rho + \frac{1}{3h^2}\right)\left(\frac{\mathrm{d}\eta}{\mathrm{d}X}\right)^2 + \left(\rho\eta + \frac{1}{3h}\right)\frac{\mathrm{d}^2\eta}{\mathrm{d}X^2} + \rho\frac{\mathrm{d}}{\mathrm{d}X}H\left[\eta\frac{\mathrm{d}}{\mathrm{d}X}H[\eta]\right] + \frac{1}{2}\rho\left\{\frac{\mathrm{d}}{\mathrm{d}X}H[\eta]\right\}^2. \quad (5.8)$$

If $O(\mu^2)$ terms are neglected, then (5.7) becomes

$$-\frac{\eta}{U^2} + \frac{1}{2(1-\eta)^2} - \frac{1}{2} - \mu\rho H[\eta_X] = 0. \quad (5.9)$$

Let for $U = U^{(0)}$ the solution of (5.9) for η be $\eta^{(0)}(X)$, i.e. $\eta^{(0)}(X)$ satisfies the equation,

$$-\frac{\eta^{(0)}}{U^{(0)2}} + \frac{1}{2(1-\eta^{(0)})^2} - \frac{1}{2} - \mu\rho H\left[\eta_X^{(0)}\right] = 0. \quad (5.10)$$

Now let

$$\eta = \eta^{(0)}(X) + \mu^2\eta^{(1)}(X) \quad (5.11)$$

be the solution of (5.7) with $U = U^{(0)}$, where $\eta^{(0)}(X)$ satisfies (5.10). Substituting for η given by (5.11) in (5.7) with $U = U^{(0)}$ and then equating $O(\mu^2)$ terms on both sides, the following equation is obtained determining $\eta^{(1)}(X)$,

$$\left[-\frac{1}{U^{(0)2}} + \frac{1}{(1-\eta^{(0)})^3} - \mu\rho\partial_X H\right]\eta^{(1)} = F\left(\eta^{(0)}, \eta_X^{(0)}, \eta_{XX}^{(0)}\right). \quad (5.12)$$

Finally, if we normalize X by h_1 instead of by L, according to (2.1), we have $\mu = 1$ and consequently we find that

$$\eta = \eta^{(0)}(X) + \eta^{(1)}(X) \quad (5.13)$$

is the solution of the following equation for $U = U^{(0)}$,

$$-\frac{\eta}{U^2} + \frac{1}{2(1-\eta)^2} - \frac{1}{2} - \rho H[\eta_X] = F(\eta, \eta_X, \eta_{XX}), \quad (5.14)$$

where $\eta^{(0)}(X)$ satisfies the equation

$$-\frac{\eta}{U^2} + \frac{1}{2(1-\eta)^2} - \frac{1}{2} - \rho H[\eta_X] = 0 \quad (5.15)$$

for $U = U^{(0)}$, and $\eta^{(1)}(X)$ is obtained from the equation

$$\left[-\frac{1}{U^{(0)2}} + \frac{1}{(1-\eta^{(0)})^3} - \rho\partial_X H\right]\eta^{(1)} = F\left(\eta^{(0)}, \eta_X^{(0)}, \eta_{XX}^{(0)}\right). \quad (5.16)$$

Equation (5.15) is same as (13) of Choi & Camassa (1996*b*) and (4.46) of Choi & Camassa (1999). Therefore, having obtained the solution of (5.15) for $U = U^{(0)}$ by Newton's method following Choi & Camassa (1996*b*) or Choi & Camassa (1999), we can get $\eta^{(1)}(X)$ from (5.16). This gives solitary wave solutions (5.13) for long internal waves in a two-fluid system for different wave speeds.

The method of Choi & Camassa (1996*b*) for solving their equation (13) is applied here to recompute the solution $\eta^{(0)}(X)$ of (5.15) for two different values of $U = 1.20$,

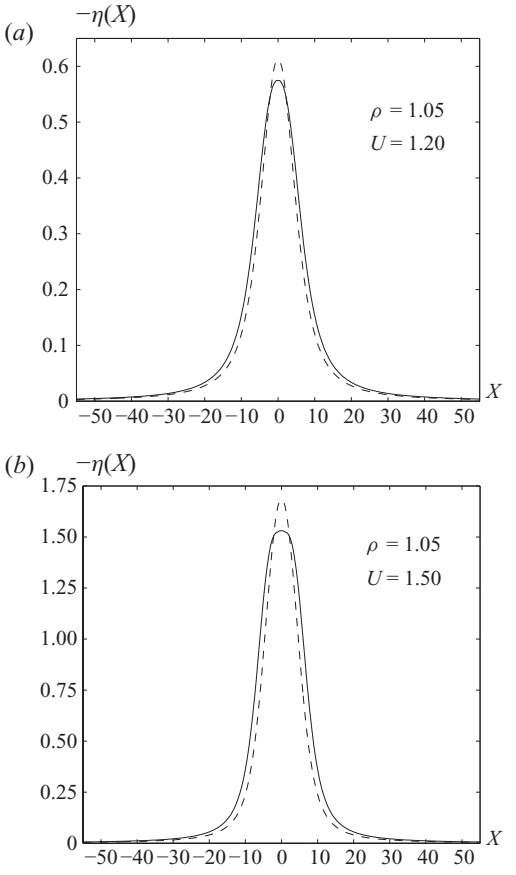

FIGURE 3. Comparison of $O(\mu)$ wave profile and $O(\mu^2)$ wave profile; $\rho = 1/R = 1.05$. (*a*) $U = 1.20$, (*b*) $U = 1.50$. - - - - - - $O(\mu)$ wave profile; ——— $O(\mu^2)$ wave profile.

1.50 and for $\rho = 1.05$, 1.28 choosing

$$\eta^{(0)}(X) = -\frac{\alpha}{1 + \dfrac{9\alpha^2 X^2}{16\rho}}, \quad U = 1 + \frac{3}{8}\alpha, \tag{5.17}$$

which is the solution of BO equation, as the initial guess. The numerical scheme is given in detail in Choi & Camassa (1996*b*). Here we have followed the same scheme. We take $\rho = 1.05$, 1.28 and $U = 1.20$, 1.50. Substituting this solution $\eta^{(0)}(X)$ on the right-hand side of (5.16) we solve this equation for $\eta^{(1)}(X)$ with the same kind of discretization as for solving (5.15). The solitary wave profile $\eta(X) = \eta^{(0)}(X) + \eta^{(1)}(X)$ for two different values of U and two different values of ρ are shown in figure 3(a, b) and figure 4(a, b) showing profiles correct to both $O(\mu)$ and $O(\mu^2)$ terms.

Finally, we plot $-\eta(0)$, the maximum depression of solitary wave profile against U, the solitary wave speed in figure 5.

In figure 3(a, b) and figure 4(a, b) solitary wave profiles are for fixed value of velocity. We have also plotted solitary wave profiles obtained from (5.7) and (5.9) for fixed value of amplitude. These are shown in figure 6(a, b). It is observed that at $O(\mu^2)$ order solitary wave crest becomes flattened and it is more clear for larger amplitudes.

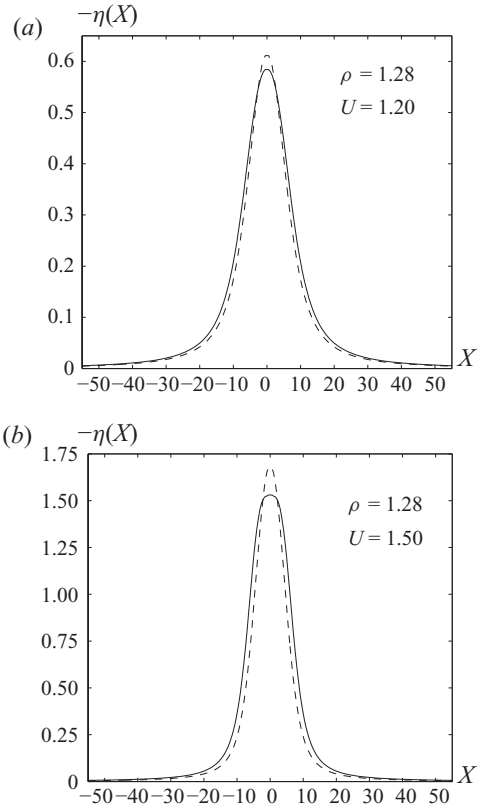

FIGURE 4. Comparison of $O(\mu)$ wave profile and $O(\mu^2)$ wave profile; $\rho = 1/R = 1.28$. (*a*) $U = 1.20$, (*b*) $U = 1.50$. - - - - - - $O(\mu)$ wave profile; ——— $O(\mu^2)$ wave profile.

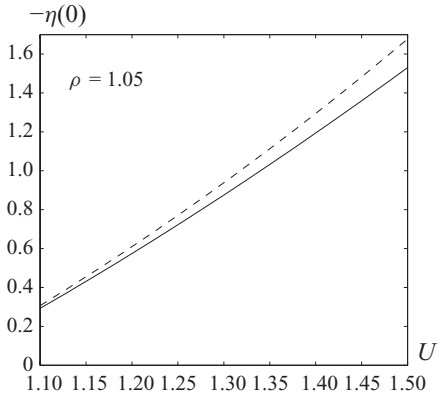

FIGURE 5. Maximum depression $-\eta(0)$ against velocity U; $\rho = 1/R = 1.05$; - - - - - - for $O(\mu)$ equation; ——— for $O(\mu^2)$ equation.

To compare solitary wave profiles obtained numerically from $O(\mu^2)$ evolution equation (5.7) with the wave profiles obtained from full Euler equations algorithm (shown in Grue *et al.* 1999) we have plotted figure 7(*a*, *b*) for $\rho^{-1} = R = 0.78$ and for two different values of wave amplitude a_m. In figure 7(*a*) Euler's wave profile is for the case when the depth ratio of the upper fluid layer to the lower fluid layer

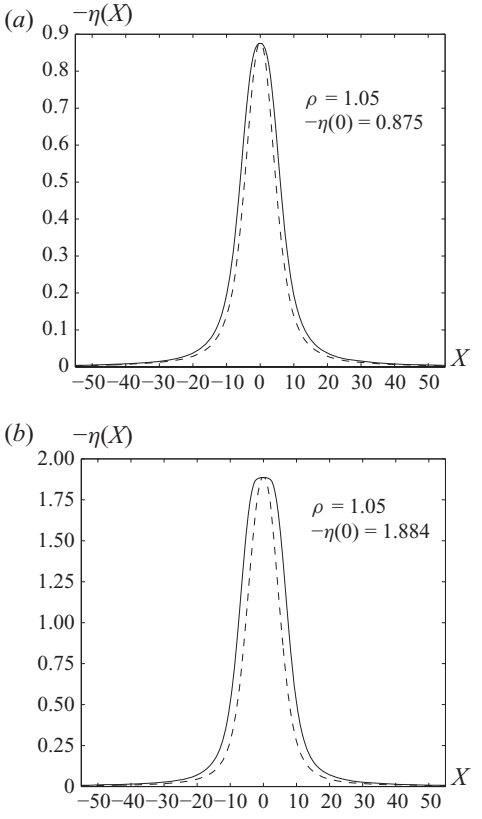

FIGURE 6. Comparison of $O(\mu)$ wave profile and $O(\mu^2)$ wave profile; $\rho = 1.05$; - - - - - - $O(\mu)$ wave profile; ——— $O(\mu^2)$ wave profile.

is 1:9 and in figure 7(b) the depth ratio is 1:24. Solitary wave profiles as obtained from $O(\mu)$ evolution equation (5.9) are also plotted in figure 7(a, b). These figures show that $O(\mu^2)$ evolution equation (5.7) gives more appropriate results than $O(\mu)$ evolution equation (5.9).

Figure 8 shows a comparison of solitary wave amplitude against velocity as estimated from $O(\mu)$ evolution equation (5.9), $O(\mu^2)$ evolution equation (5.7) and also from Euler's estimate by taking the depth ratio 1:99 (figure 10b of Camassa *et. al.* 2006). It is found that as far as solitary wave amplitude is concerned, the $O(\mu^2)$ evolution equation (5.7) predicts almost accurately the solitary wave amplitude provided that the lower fluid is deep enough and velocity is small enough.

6. A time-domain solution for weakly nonlinear case

As a simplest time-domain solution of (3.4) and (3.5) in the weakly nonlinear case we consider the propagation of an approximate solitary wave following the numerical method given by Nguyen & Dias (2008).

If in (2.1) we take $U_0 = \sqrt{gh_1(1-R)/R}$ instead of $U_0 = \sqrt{gh_1}$ then (3.4) and (3.5) assume the following forms:

$$\left(\frac{1-R}{R}\right)\eta_t = (hu)_x - \frac{1}{2}\mu^2\left\{h\left(\frac{h^2}{3} - B_2\right)u_{xx}\right\}_x \tag{6.1}$$

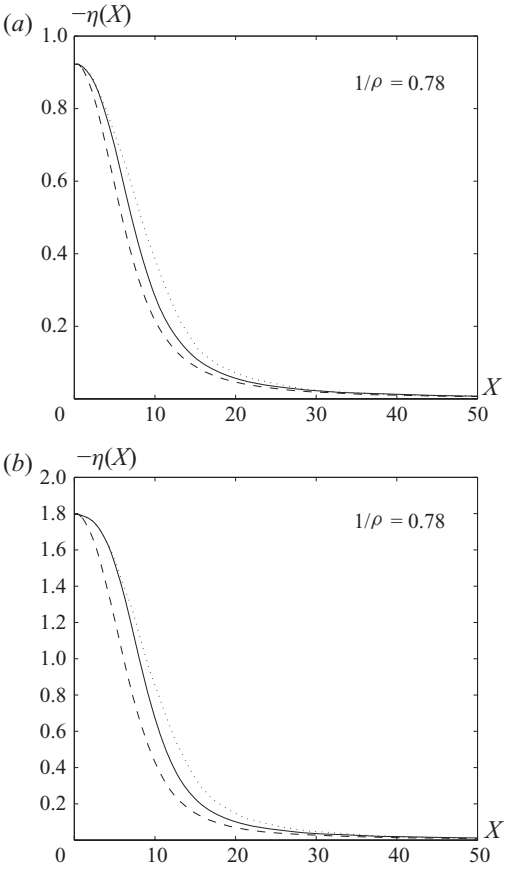

FIGURE 7. Comparison of $O(\mu)$ wave profile and $O(\mu^2)$ wave profile with Euler's result; $\rho^{-1} = 0.78$; (*a*) $h_1{:}h_2 = 1{:}9$; $-\eta(0) = .92246$; (*b*) $h_1{:}h_2 = 1{:}24$; $-\eta(0) = 1.7955$; ..... Euler equation solution (Camassa *et al.* 2006); - - - - - $O(\mu)$ wave profile; ——— $O(\mu^2)$ wave profile.

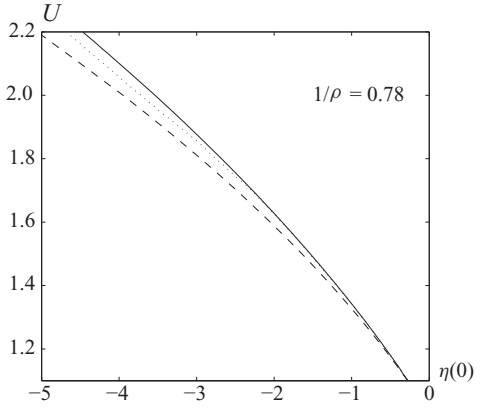

FIGURE 8. Velocity U versus amplitude $\eta(0)$ of solitary wave profile; $R = \rho^{-1} = 0.78$; Euler equations result (Camassa *et al.* 2006) for $h_1{:}h_2 = 1{:}99$ (dotted line); $O(\mu)$ wave profile (dashed line); $O(\mu^2)$ wave profile (solid line).

and

$$\left(\frac{R}{1-R}\right)u_t = \eta_x - \epsilon\left(\frac{R}{1-R}\right)^2 uu_x + \frac{\mu}{R}H[\eta_{tt}] + \frac{\mu^2\epsilon}{R}\eta_t\eta_{xt} + \frac{\mu^2\epsilon}{R}(\eta\eta_{tt})_x + \frac{1}{2}\mu^2\left(\frac{R}{1-R}\right)\{(h^2-B_2)u_{xt}\}_x + \frac{1}{2}\mu^2\epsilon\left(\frac{R}{1-R}\right)^2\{(h^2-B_2)uu_{xx}\}_x - \frac{1}{2}\mu^2\epsilon\left(\frac{R}{1-R}\right)^2\{h^2u_x^2\}_x + \frac{\mu^2\epsilon}{R}H[\{\eta_t H[\eta_t]\}_x] + \frac{\mu^2\epsilon}{R}H[\{\eta H[\eta_{tt}]\}_x] + \frac{\mu^2\epsilon}{R}H[\eta_t]\{H[\eta_t]\}_x. \tag{6.2}$$

Equations (6.1) and (6.2) can be directly employed to find a time-domain solution. Instead of doing so, here we derive a single time-evolution equation for one-way propagation and then we apply the Runge–Kutta–Gill algorithm to perform time stepping. This reduces computational time and effort considerably. For derivation of single time-evolution equation we have followed the technique of Nguyen & Dias (2008).

For travelling wave solution of (6.1) and (6.2) in the form $\eta = \eta(x - Ut)$ and $u = u(x - Ut)$, where U is slightly greater than 1 for right travelling wave, we take $u = u(\eta)$ up to $O(\mu^2)$ as follows:

$$u = -\left(\frac{1-R}{R}\right)(\eta + M + \mu N + \mu^2 S), \tag{6.3}$$

where M, N, S are correct to $O(\epsilon^2)$ satisfying $M_t \approx -M_x$, $N_t \approx -N_x$ and $S_t \approx -S_x$ for right travelling wave of sufficiently small amplitude. Expressions for M, N and S are given in Appendix B.

For u given by (6.3), the time-evolution equation at $O(\mu)$ becomes

$$\eta_t + \left\{\eta - \frac{3}{4}\epsilon\eta^2 + \frac{\mu}{2R}H[(1-3\epsilon\eta)\eta_x] - \frac{\mu}{2R}\epsilon\eta H[\eta_x]\right\}_x = 0. \tag{6.4}$$

For solitary wave solution of (6.4) propagating towards positive x direction with velocity U, (6.4) gives

$$-U\eta + \eta - \frac{3}{4}\epsilon\eta^2 + \frac{\mu}{2R}H[(1-3\epsilon\eta)\eta_x] - \frac{\mu}{2R}\epsilon\eta H[\eta_x] = 0. \tag{6.5}$$

Equation (6.5) matches with (5.9) up to $O(\epsilon^2)$ when the term $1/h^2$ of it expanded binomially and U of (6.5) is replaced by $((3/2) - (1/2U^2))$.

We now apply Newton's method to (6.5) in order to find a solitary wave profile satisfying (6.5) for $U = 1.1$. For this, we have chosen the initial profile to be

$$\eta^{(0)} = \eta(x - Ut) = -\frac{\alpha}{1 + \dfrac{9\alpha^2(x-Ut)^2}{16\rho}}, \quad \alpha = \frac{8}{3}\left(\frac{1}{\sqrt{3-2U}} - 1\right). \tag{6.6}$$

While applying Newton's method to (6.5), we have chosen the x interval as [−400, 1600] and partitioned it by the points $x_i = x_0 + ie, i = (1)n$, where $x_0 = -400$, $x_n = +1600$ and $e = 0.5$. Denoting η at x_i by η_i we can write (6.5) in discretized form as follows:

$$-U\eta_i + \eta_i - \frac{3}{4}\eta_i^2 + \frac{1}{2R}\{H[(1-3\eta)\eta_x]\}_i - \frac{1}{2R}\eta_i\{H[\eta_x]\}_i = 0, \qquad i = 1(1)n. \tag{6.7}$$

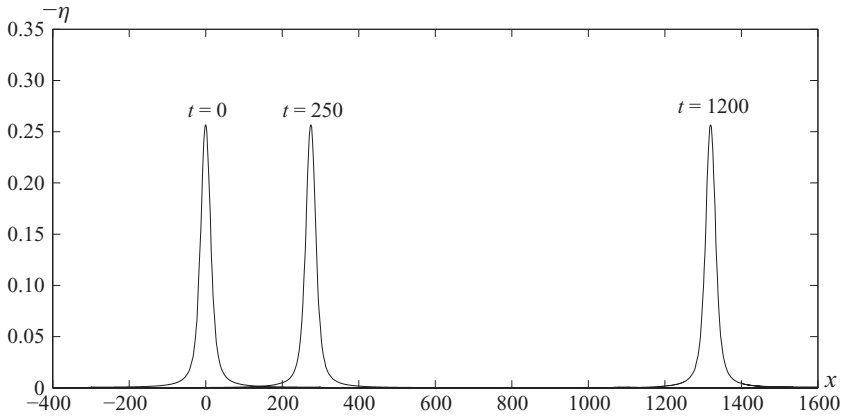

FIGURE 9. Solitary wave propagating with velocity $U = 1.104$; $\rho = 1/R = 1.28$.

The associated Jacobian matrix is given by $[JAC_{ij}]$, where

$$JAC_{ij} = \left[-U + 1 - \frac{3}{2}\eta - \frac{1}{2R}\{H[\eta_x]\}_i \right]\delta_{ij} + \frac{1}{2R\pi e}\left\{ \frac{\omega_{j-1}}{j-i-.5} - \frac{\omega_j}{j-i+.5} \right\}\{(1-3\eta_j) - \eta_i\},\ i, j = 1(1)n, \quad (6.8)$$

where $\omega_j = .5$ for $j = 1, n$, otherwise $\omega_j = 1$. These are the quadrature weights when the Hilbert transform term is replaced by a composite Trapezoidal rule. All other Hilbert transform terms are evaluated using the property $F(Hf)(\xi) = -i\ \mathrm{sgn}(\xi)F(f)(\xi)$, where F denotes the Fourier transform. For numerical computation of such terms, the fast Fourier transform and its inverse transform are applied.

Finally, at order $O(\mu^2)$, we get the following time-evolution equation:

$$\eta_t + \left\{ \eta - \frac{3}{4}\epsilon\eta^2 + \frac{\mu}{2R}H[(1-3\epsilon\eta)\eta_x] - \frac{\mu}{2R}\epsilon\eta H[\eta_x] + \mu^2 S - \mu^2\epsilon\left(\frac{1}{3} - \frac{B_2}{2} - \frac{1}{2R^2}\right)\eta\eta_{xx} \right\}_x = 0. \quad (6.9)$$

Equation (6.9) is correct up to $O(\mu^2, \epsilon^2)$. We then find approximate solitary wave profile satisfying (6.9) by improving the wave profile obtained from (6.5). For this we have followed the same procedure explained in § 5. In order to observe the time evolution of this solitary wave just obtained we apply Runge–Kutta–Gill algorithm to (6.9). While applying Runge–Kutta–Gill algorithm we have taken time step to be $\delta t = 0.01$. We find that the wave retains its initial shape while moving along positive x direction for a long time. The wave profiles at $t = 0$, 250 and 1200 are shown in figure 9.

7. Conclusion

Choi & Camassa (1996*b*, 1999) have derived fully nonlinear $O(\mu)$ model equations for internal waves in a two-fluid system with deep lower layer. In the present paper, these equations have been extended to include $O(\mu^2)$ terms and to include the effect of propagation in two horizontal space dimensions. The model equations derived consist of two coupled equations for two dependent variables, one of which is the

elevation of the interface and the other is the horizontal velocity in the upper layer at an arbitrary elevation, while in Choi & Camassa (1996*b*, 1999) this variable is the depth averaged velocity. For unidirectional solitary wave propagation the two coupled equations reduce to a single equation for the elevation of the interface. It is shown that this single equation can be solved by the same numerical method adopted by Choi & Camassa (1996*b*, 1999). For two values of density ratios and for two different wave speeds the solitary wave profiles have been obtained numerically. Figures have been plotted showing amplitude against velocity for two different density ratios. It is found that the amplitude increases with velocity. It is also observed that the peak amplitude according to $O(\mu^2)$ equation is lower than that from $O(\mu)$ equation. It is found that solitary wave profiles obtained from $O(\mu^2)$ evolution equation are in better agreement with Euler's computational profiles than those from $O(\mu)$ evolution equation. The propagation of solitary wave is also studied numerically.

For application in real oceans, the assumption of constant density layers cannot be very accurate and it is necessary to consider more realistic density profiles. By approximating a realistic density profile by a number of layers of different constant buoyancy frequency, the Helmholtz equation can easily be solved in each layer although two neighbouring layers are coupled nonlinearity through boundary conditions at the interfaces. Using such type of density profile, Grue *et al.* (2000) and Fructus & Grue (2004), respectively, for two and three layer systems computed numerically the fully nonlinear solution of Euler equations. Vornovich (2003), on the other hand, used a long wave asymptotic approach similar to Choi & Camassa (1999) and obtained a strongly nonlinear model for a two-layer system with constant buoyancy frequency in each layer and a possible jump in density at the layer interface. Goullet & Choi (2008) have further considered the more restricted case with a continuous density distribution at the interface. We are presently investigating higher-order model equations in this context for the case of finite water depth. Results will be described in a subsequent paper.

This collaborative work started while one of the authors (K. P. Das) was a visitor at the Center for Applied Coastal Research, University of Delaware. This author is grateful for the hospitality during that period. This work was partially supported by the College of Engineering, University of Delaware.

Appendix A. Derivation of linear dispersion relation

If we assume $\eta = \eta_0 e^{i(\boldsymbol{k}.\boldsymbol{r}-\omega t)}$, where η_0 is a constant, then the second term of (4.7)

$$= -\frac{1}{2\pi}\mu\omega^2 e^{-i\omega t}\eta_0\nabla^2 \int\int_{-\infty}^{\infty} \frac{1}{|\xi|} e^{i\boldsymbol{k}.(\boldsymbol{r}+\xi)}\, d\xi, \qquad \boldsymbol{r}-\boldsymbol{r}' = \xi,$$
$$= \mu\omega^2 k\eta.$$

Therefore, if the space–time dependence of η and P_a is of the form $e^{i(\boldsymbol{k}.\boldsymbol{r}-\omega t)}$, then we get the following two algebraic equations from (4.5) and (4.7)

$$i\omega\eta + \left\{1 + \frac{1}{2}\mu^2\left(\frac{1}{3} - B_2\right)k^2\right\}P_a = 0,$$
$$\{k^2(1-R) - \mu\omega^2 k\}\eta - i\omega R\left\{1 + \frac{1}{2}\mu^2(1-B_2)k^2\right\}P_a = 0.$$

The condition for the existence of nontrivial solution of these two equations for η and P_a produces the linear dispersion given by (4.8).

Appendix B. Derivation of M, N and S appearing in (6.3)

At $O(\mu^0)$, (6.1) and (6.2) reduce to the following equations:

$$\left(\frac{1-R}{R}\right)\eta_t = (hu)_x, \tag{B 1}$$

$$\left(\frac{R}{1-R}\right)u_t = \eta_x - \epsilon\left(\frac{R}{1-R}\right)^2 uu_x. \tag{B 2}$$

To find single time-evolution equation for sufficiently small-amplitude waves we take (following Nguyen & Dias 2008)

$$u = -\left(\frac{1-R}{R}\right)(\eta + \epsilon M), \tag{B 3}$$

where M is small compared to η and u and satisfy $M_t \approx -M_x$ for right travelling waves. Either of the two equations (B 1) and (B 2) produce the same evolution equation

$$\eta_t + \left\{\eta - \frac{3}{4}\epsilon\eta^2\right\}_x = 0, \tag{B 4}$$

if $M = \epsilon\eta^2/4$. At $O(\mu)$, we take

$$u = -\left(\frac{1-R}{R}\right)(\eta + \epsilon M + \mu N), \tag{B 5}$$

where N is correct to $O(\epsilon^2)$ and $N_t \approx -N_x$. Equations (6.1) and (6.2) produce the same evolution equation (6.5) if N has the following form:

$$N = \frac{1}{2R}H[(1-3\epsilon\eta)\eta_x]. \tag{B 6}$$

While finding N we have calculated η_{tt} using (B4) as follows:

$$\eta_{tt} = -\left\{\eta - \frac{3}{4}\epsilon\eta^2\right\}_{tx} = (1-3\epsilon\eta)\eta_{xx} - 3\epsilon\eta_x^2. \tag{B 7}$$

Extending the analysis up to $O(\mu^2)$ in a similar way, we get

$$\begin{aligned} S = {} & \left(\frac{1}{3} - \frac{B_2}{2} - \frac{1}{2R^2}\right)\eta_{xx} - \frac{\epsilon}{4}(1-B_2)\eta\eta_x + \frac{\epsilon}{4}\left(\frac{1}{R} - \frac{5}{6} - \frac{B_2}{2} + \frac{15}{2R^2}\right)\eta_x^2 \\ & + \frac{\epsilon}{2}\left(\frac{1}{R} - \frac{11}{2} - \frac{B_2}{4} + \frac{15}{4R^2}\right)\eta\eta_{xx} + \frac{\epsilon}{2}\left(\frac{1}{R} - \frac{1}{R^2}\right)H[\eta_x H[\eta_x]] \\ & + \frac{\epsilon}{2}\left(\frac{1}{R} - \frac{7}{4R^2}\right)H[\eta H[\eta_{xx}]] + \frac{\epsilon}{4}\left(\frac{1}{R} - \frac{1}{4R^2}\right)\{H[\eta_x]\}^2. \end{aligned} \tag{B 8}$$

While calculating S we have calculated η_t and η_{tt} from (6.5).

REFERENCES

Bingham, H. B. & Agnon, Y. 2005 A Fourier–Boussinesq method for nonlinear water waves. *Eur. J. Mech.* B **24**, 255–274.

Camassa, R., Choi, W., Michallet, H., Russas, P.-O. & Sveen, J. K. 2006 On the realm of validity of strongly nonlinear asymptotic approximations for internal wave. *J. Fluid Mech.* **549**, 1–23.

Choi, W. & Camassa, R. 1996*a* Weakly nonlinear internal waves in a two-fluid system. *J. Fluid Mech.* **313**, 83–113.

Choi, W. & Camassa, R. 1996*b* Long internal waves of finite amplitude. *Phys. Rev. Lett.* **77**, 1759–1762.

Choi, W. & Camassa, R. 1999 Fully nonlinear internal waves in a two-fluid system. *J. Fluid Mech.* **396**, 1–36.

Clamond, D. & Grue, J. 2001 A fast method for fully nonlinear water-wave computations. *J. Fluid Mech.* **447**, 337–355.

Fructus, D. & Grue, J. 2004 Fully nonlinear solitary waves in a layered stratified fluid. *J. Fluid Mech.* **505**, 323–347.

Gobbi, M. F., Kirby, J. T. & Wei, G. E. 2000 A fully nonlinear Boussinesq model for surface waves. Part 2. Extension to $O((kh)^4)$. *J. Fluid Mech.* **405**, 181–210.

Goullet, A. & Choi, W. 2008 Large amplitude internal solitary waves in a two-layer system of piecewise linear stratification. *Phys. Fluids* **20**, 096601.

Grue, J. 2002 On four highly nonlinear phenomena in wave theory and marine hydrodynamics. *Appl. Ocean Res.* **24**, 261–274.

Grue, J., Jensen, A., Rusas, P.-O. & Sveen, J. K. 1999 Properties of large-amplitude internal waves. *J. Fluid Mech.* **380**, 257–278.

Grue, J., Jensen, A, Rusas, P.-O. & Sveen, J. K. 2000 Breaking and broadening of internal solitary waves. *J. Fluid Mech.* **413**, 181–217.

Helfrich, K. R. & Melville, W. K. 2006 Long nonlinear internal waves. *Annu. Rev. Fluid Mech.* **38**, 395–425.

Jackson, C. R. 2004 An atlas of internal solitary-like waves and their properties. http://www.internalwaveatlas.com/Atlas2.index.html.

Koop, C. G. & Butler, G. 1981 An investigation of internal solitary waves in a two-fluid system. *J. Fluid Mech.* **112**, 225–251.

Liu, A. K., Chang, Y. S., Hsu, M. K. & Liang, N. K. 1998 Evolution of nonlinear internal waves in the East and South China Seas. *J. Geophys. Res.* **103**, 7995–8008.

Lynett, P. J. & Liu, P. L. F. 2002 A two-dimensional depth-integrated model for internal wave propagation over variable bathymetry. *Wave Motion* **36**, 221–240.

Madsen, P. A., Bingham, H. B. & Liu, H. 2002 A new Boussinesq method for fully nonlinear waves from shallow to deep water. *J. Fluid Mech.* **462**, 1–30.

Nguyen, H. Y. & Dias, F. 2008 A Boussinesq system for two-way propagation of interfacial waves. *Physica* D **237**, 2365–2389.

Nwogu, O. 1993 An alternative form of Boussinesq equations for nearshore wave of Boussinesq equations for nearshore wave propagation. *J.Waterway Port Coast. Ocean Engng* **119**, 618–638.

Orr, M. H. & Mignerey, P. C. 2003 Nonlinear internal waves in south China sea: Observation of the conservation of the depression internal waves, *J. Geophys. Res.* **108** (C3), 3064, doi:10.1029/2001JC001163.

Ostrovsky, L. A. & Grue, J. 2003 Evolution equations for strongly nonlinear internal waves. *Phys. Fluids* **15** (10), 2934–2948.

Phillips, O. M. 1977 *Dynamics of the Upper Ocean.* Cambridge University Press.

Ruiz de Zárate, A., Vigo, D., Nachbin, A. & Choi, W. 2009 A higher-order internal wave model accounting for large bathymetric variations. *Stud. Appl. Math.* **122**, 275–294.

Segur, H. & Hammack, J. L. 1982 Soliton models of long internal waves. *J. Fluid Mech.* **118**, 285–304.

Stanton, T. P. & Ostrovsky, L. A. 1998 Observation of highly nonlinear internal solitons over the continental shelf. *Geophys. Res. Lett.* **25**, 2695–2698.

Voronovich, A. G. 2003 Strong solitary internal waves in a 2.5 layer model. *J. Fluid Mech.* **474**, 85–94.

Wei, G., Kirby, J. T., Grilli, S. T. & Subramanya, R. 1995 A fully nonlinear Boussinesq model for surface waves. Part 1. Highly nonlinear unsteady waves. *J. Fluid Mech.* **294**, 71–92.

Zeng, K. & Alpers, W. 2004 Generation of internal solitary waves in Sulu Sea and their refraction by bottom topography studied by ERS SAR imagery and numerical model. *Intl J. Remote Sens.* **25**, 1277–1281.